Hydrogen adsorbed in a metal organic framework-5: Coupled translation-rotation eigenstates from quantum five-dimensional calculations

Ivana Matanović, Jonathan L. Belof, Brian Space, Kaido Sillar, Joachim Sauer et al.

Additional information on J. Chem. Phys.

Hydrogen adsorbed in a metal organic framework-5: Coupled translation-rotation eigenstates from quantum five-dimensional calculations

Ivana Matanović,[1,a)] Jonathan L. Belof,[2,3] Brian Space,[3] Kaido Sillar,[4] Joachim Sauer,[4] Juergen Eckert,[5] and Zlatko Bačić[6,b)]

[1]*Theoretical Division, Los Alamos National Laboratory, Los Alamos, New Mexico 87545, USA*
[2]*Lawrence Livermore National Laboratory, 7000 East Avenue, Livermore, California 94550, USA*
[3]*Department of Chemistry, University of South Florida, 4202 East Fowler Avenue, CHE205, Tampa, Florida 33620-5250, USA*
[4]*Institut für Chemie, Humboldt-Universität zu Berlin, Germany*
[5]*Materials Research Laboratory, University of California, Santa Barbara, California 93106, USA*
[6]*Department of Chemistry, New York University, New York 10003, USA*

We report rigorous quantum five-dimensional (5D) calculations of the coupled translation-rotation (T-R) eigenstates of a H_2 molecule adsorbed in metal organic framework-5 (MOF-5), a prototypical nanoporous material, which was treated as rigid. The anisotropic interactions between H_2 and MOF-5 were represented by the analytical 5D intermolecular potential energy surface (PES) used previously in the simulations of the thermodynamics of hydrogen sorption in this system [Belof *et al.*, J. Phys. Chem. C **113**, 9316 (2009)]. The global and local minima on this 5D PES correspond to all of the known binding sites of H_2 in MOF-5, three of which, α-, β-, and γ-sites are located on the inorganic cluster node of the framework, while two of them, the δ- and ϵ-sites, are on the phenylene link. In addition, 2D rotational PESs were calculated *ab initio* for each of these binding sites, keeping the center of mass of H_2 fixed at the respective equilibrium geometries; purely rotational energy levels of H_2 on these 2D PESs were computed by means of quantum 2D calculations. On the 5D PES, the three adjacent γ-sites lie just 1.1 meV above the minimum-energy α-site, and are separated from it by a very low barrier. These features allow extensive wave function delocalization of even the lowest translationally excited T-R eigenstates over the α- and γ-sites, presenting significant challenges for both the quantum bound-state calculations and the analysis of the results. Detailed comparison is made with the available experimental data. © *2012 American Institute of Physics*. [http://dx.doi.org/10.1063/1.4730906]

I. INTRODUCTION

Establishing hydrogen as the clean energy carrier of the future depends critically on the development of new materials that can store large amounts of hydrogen economically, safely, reversibly, and under moderate, near-ambient conditions.[1,2] The approach to storing hydrogen by physisorption inside nanoporous materials has been the subject of a great deal of research activity in recent years.[1,3,4] Progress in the design and creation of an effective porous material that could be of practical use as a sorption-based hydrogen storage medium would be greatly aided by developing a detailed, molecular-level understanding of the interaction of molecular hydrogen at the wide range of binding sites that may be encountered in nanoporous materials, particularly in metal organic frameworks (MOFs). A great deal of effort has therefore been made to obtain potential energy surfaces (PESs) of sufficient accuracy for the simulation of adsorption properties such as isotherms and the isosteric heats of adsorption.[5–8] The interactions responsible for these properties, however, probe only the minima on the global PES for hydrogen molecule(s) in a particular system, which may therefore not be adequately tested by simply accounting for experimentally determined adsorption isotherms. Moreover, thermodynamic measurements average over all H_2 binding sites that are occupied at a particular loading, and hence do not give direct site-specific information.

Common molecular-level experimental probes which utilize photons (e.g., optical spectroscopy, x-ray diffraction) are not very sensitive to hydrogen because of the very small number of electrons in the molecule. Neutrons, on the other hand, interact much more strongly with hydrogen than any other element,[9] and are therefore highly selective probes of adsorbed H_2; they can be used both for structural studies (diffraction)[10,11] and spectroscopy (inelastic scattering). In addition, neutrons have the ability to change the total nuclear spin I of the hydrogen molecule, something which photons cannot do. This makes it possible to observe the rotational $\Delta J = 1$ transitions, such as $J = 0 \rightarrow 1$ of *para*-H_2 ($I = 0$) and $J = 1 \rightarrow 2$ of *ortho*-H_2 ($I = 1$). $\Delta J =$ odd transition are forbidden in optical, infrared (IR) and Raman spectroscopy of H_2, since they involve the *ortho-para* conversion.

a)Also at R. Bošković Institute, Department of Physical Chemistry, Bijenička 54, 10000 Zagreb, Croatia. Electronic mail: ivana@lanl.gov.
b)Electronic mail: zlatko.bacic@nyu.edu.

Because of these unique advantages, inelastic neutron scattering (INS) spectroscopy has been widely employed to study the fundamental properties of molecular hydrogen confined within the nanoscale cavities of diverse materials,[12,13] including fullerenes,[14–16] clathrate hydrates,[17,18] MOFs,[19–23] zeolites,[24–26] nanostructured carbon,[27,28] and alkali-metal graphite intercalation compounds.[29] The measured INS spectra contain a wealth of information about the excitations of H_2 center-of-mass (c.m.) translational motions as well as the rotational excitations of the hydrogen molecule at various binding sites, and through this, about the potential interactions of the guest molecule with the host material. However, until the recent significant advances described later in this paper, most of this information could not be extracted with confidence, owing to the inherent limitations of the approximate, reduced-dimensionality theoretical approaches used to analyze the INS spectra. In a number of INS studies of molecular hydrogen adsorbed in various nanoporous materials,[19–21,25–28] efforts were made to interpret the spectra with the aid of phenomenological models for the rotational potential, which assume that translational and rotational excitations of H_2 are separable, uncoupled. Some of the peaks in the spectra could be assigned tentatively to the rotational excitations of H_2 at different binding sites by comparing their energies to the eigenvalues of the phenomenological model, and estimates of the site-specific rotational barrier heights were obtained. However, since this type of model includes neither the H_2 translational excitations nor the coupling between its translational and rotational motions, the assignments of spectral features based on it are inevitably inconclusive and incomplete. In particular, it is not possible to resolve the ambiguity of differentiating between transitions that are translational or rotational in nature, or a combination of both.

A much more definitive and comprehensive analysis and assignment of the experimental INS spectra require a rigorous treatment of the five-dimensional (5D) quantum dynamics of the nanoconfined H_2 molecule, in which its three translational and the two rotational degrees of freedom (DOFs) are treated as fully coupled, on an accurate 5D PES. A partial step in this direction was made in the recent theoretical investigations of H_2 in two different MOFs, HKUST-1 (Ref. 22) and MOF-74,[30] although the H_2 translations and rotations were taken to be uncoupled. In both studies, 2D angular PESs were determined using density functional theory (DFT) calculations, for the H_2 c.m. fixed at one or two binding sites, and the rotational energy levels were calculated on them. Moreover, after fixing the H_2 orientation, 1D translational potential curves were also calculated using DFT along certain directions, for which the energy levels were calculated. The approximate rotational and translational transition frequencies obtained in this way were used in the efforts to assign the measured INS spectra. However, the assignments were complicated by the fact that in both systems the calculated translational and rotational energy levels turned out to be close in energy.[22,30] This also indicated that the assumption of the separability of the rotational and translational DOFs of H_2 in these MOFs is not justified, and that excitation energies computed in this approximation are likely to be significantly inaccurate.

In fact, as a result of recent developments, when studying the quantum behavior of H_2 in MOFs it is no longer necessary to rely on reduced-dimension treatments which neglect the translation-rotation (T-R) coupling. An effective and general methodology for accurate quantum calculation of the fully coupled 5D T-R energy levels and wave functions of H_2/HD/D_2 molecule inside an arbitrarily shaped nanoscale cavity (assumed to be rigid) has been available for several years.[31] It was initially developed and implemented for the purpose of investigating the quantum 5D T-R dynamics of a hydrogen molecule encapsulated in the small[31,32] and large cages[33] of the structure II (sII) clathrate hydrate. Subsequently, this methodology was used to calculate the 5D T-R eigenstates of H_2/HD/D_2 inside the fullerenes C_{60},[16,34–37] C_{70},[36,37] and aza-thia-open-cage fullerene (ATOCF).[38] In every study, detailed comparison was made with all available experimental results. Given that the T-R dynamics is treated exactly, any discrepancies between theory and experiment can be attributed primarily to some deficiencies of the 5D PES employed, thus providing a stringent test of its quality. In the case of H_2/HD in the small cage of sII clathrate hydrate[32] and H_2 in ATOCF,[38] the fully coupled T-R excitation energies from the quantum 5D calculations were compared to the measured INS spectra,[14,17] helping with the interpretation of the observed rotational and translational excitations and assessing the accuracy of the respective PESs.

The quantum 5D calculations described above, while a major improvement over the reduced-dimension approaches used in the past, do not remove completely the ambiguities in the assignment of the experimental INS spectra; since they do not provide information on the intensities of the computed T-R transitions, it is not clear which of these should be observable. Ideally, theory needs to provide the full spectroscopic fingerprint of the quantum T-R dynamics of the nanoconfined hydrogen molecule, by computing accurately the intensities of the INS transitions, in addition to their energies. This would make the interpretation of the measured INS spectra much more reliable and complete. In the few calculations of the INS spectra of H_2 in zeolites,[39,40] only the H_2 rotations were treated quantum mechanically; the translational motion of H_2 was assumed to be classical, which is inadequate at the low temperatures considered. Another shortcoming of such mixed quantum-classical approach is that the quantized translational excitations, alone or in combination with rotational excitations, are beyond its scope. Therefore, it misses many of the key spectral features.

The last remaining gap between the rigorous quantum theory and the experimental INS spectra of a hydrogen molecule in a nanocavity was closed only very recently. We introduced[41,42] the quantum methodology for accurate calculation of the INS spectra, i.e., the energies and intensities of the T-R transitions, of such systems, which is based on the fully coupled treatment of the quantum 5D T-R dynamics of the guest hydrogen molecule. Although our methodology takes the standard basic equations of INS theory[43,44] as the starting point, it is unique in incorporating the 5D T-R energy levels and wave functions of the entrapped H_2 molecule, rigorously calculated on the anisotropic intermolecular PES, as the initial and final states of the INS transitions.

The INS spectra simulated using this approach capture faithfully all the subtle features arising from the T-R dynamics of the guest molecule on the 5D PES of the confining environment, and therefore exhibit an unprecedented degree of realism. The power of this new methodology was first demonstrated through the simulation of the INS spectra of *para*-H$_2$ (*p*-H$_2$) and *ortho*-H$_2$ (*o*-H$_2$) in the small cage of the sII clathrate hydrate.[41] Remarkably good agreement was obtained between the computed INS spectra and the experimental data.[17] It is evident that powerful and versatile theoretical tools are now available which, for a given 5D PES, make it possible to compute numerically exact, fully coupled quantum 5D T-R energy levels and wave functions of a hydrogen molecule inside the nanocavities of host materials, including MOFs, and in the next step use them as input for the quantum calculations of highly accurate and realistic INS spectra.

MOFs are crystalline solids composed of metal nodes assembled into regular 3D lattices by polyfunctional organic linkers. They have uniform pore sizes and unusually large pore volume and surface area, which can be tuned and tailored to specific applications by exploring nearly endless combinations of different metal nodes and organic linkers. MOFs have received substantial attention in recent years because of their potential for hydrogen storage applications.[19, 20, 45–49] One of the earliest MOFs investigated for hydrogen storage is Zn$_4$O(BDC)$_3$ (known as MOF-5 or IRMOF-1),[19] in which [OZn$_4$]$^{6+}$ groups, oxygen-centered Zn$_4$ tetrahedra, are linked to an octahedral array of [O$_2$C−C$_6$H$_4$−CO$_2$]$^{2-}$ (1,4-benzenedicarboxylate, BDC) groups to form a highly porous cubic framework. MOF-5 has been widely studied as a prototypical MOF, and is currently one of the best hydrogen storage materials under cryogenic conditions (77 K).[49] It has been the subject of INS,[19–21] Raman,[50] and IR spectroscopy,[51–53] as well as the neutron diffraction measurements;[10, 11] based on them, multiple distinct adsorption sites for H$_2$ in MOF-5 have been proposed. These sites must correspond to various potential minima, global and local, of the intermolecular PES of H$_2$ in MOF-5. The available INS, IR, and Raman spectroscopic data are undoubtedly rich in information about the interaction of H$_2$ with MOF-5, which to date has not been analyzed in detail and interpreted quantitatively in terms of the underlying intermolecular PES and the multidimensional quantum T-R dynamics of H$_2$ on it. This has provided the motivation for the present work.

In this paper, we report the results of the first quantum 5D calculation of the T-R eigenstates of H$_2$ adsorbed in MOF-5, which includes full coupling between the three translational and the two rotational DOFs of the guest molecule. The recently developed analytical 5D PES[7, 54] was employed in these calculations. In addition, 2D rotational PESs were computed *ab initio*[8] for the c.m. of H$_2$ fixed at each of the four primary binding sites of MOF-5 that have been identified,[20, 55] and the H$_2$ rotational levels were calculated on them. The presence of multiple binding sites which are intricately interconnected makes the potential energy landscape for H$_2$ in MOF-5 much more complex than in the systems studied by us previously, clathrate hydrates and fullerenes. This posed major new challenges, not encountered before, to both the quantum bound-state calculations and the analysis of the results.

The theoretical results obtained are interpreted in the context of the original INS spectra for this system, as well as the additional, more recent spectroscopic information, which constitute an extremely sensitive test of the PES.

The computational methodology employed to calculate the quantum 5D T-R eigenstates of H$_2$ in the MOF, as well as its purely rotational energy levels in 2D, is briefly described in Sec. II, together with the details of the manner in which the two PESs were derived. The H$_2$ binding sites determined on the two PESs are analyzed in Sec. III A. The 2D rotational levels computed for the two PESs and the fully coupled T-R eigenstates on the 5D PES are discussed in Secs. III B and III C, respectively, followed by detailed comparison with the available experimental results in Sec. III D. Section IV contains the summary and the conclusions.

II. THEORY

A. Quantum 5D calculation of the coupled translation-rotation eigenstates

Our methodology for computing the 5D T-R energy levels and wave functions of nanoconfined hydrogen molecule has evolved over many years, starting with the computations of the 5D intermolecular vibrational eigenstates of HF in Ar$_n$HF clusters,[56, 57] in which the Ar$_n$ subunit was treated as rigid. This approach was gradually refined and eventually adapted to the problem of the quantum T-R dynamics of H$_2$ encapsulated in the cages of clathrate hydrates[31] and fullerenes.[34] Recently,[38, 58] we have implemented the basis-set contraction procedure which is at the same time simpler and more efficient than the scheme used previously. The speed, and even the feasibility, of high-dimensional bound-state calculations critically depend on the effectiveness of the basis-set contraction. Detailed presentation of our current methodology for accurate and efficient calculation of the 5D T-R eigenstates of a hydrogen molecule (H$_2$/HD/D$_2$) in nanoscale confinement, which was utilized in the present study, is given in Ref. 42. Therefore, it is only recapitulated here.

The host framework (MOF-5) is taken to be rigid and the H$_2$ bond length is held fixed. The five coordinates (x, y, z, θ, ϕ) are employed; x, y, and z are the Cartesian coordinates of the vector connecting the c.m. of H$_2$ with the center of a MOF-5 cell, while the two polar angles θ and ϕ specify the orientation of H$_2$ relative to the framework. The host framework can be safely assumed to be infinitely heavy and nonrotating. In this case, the 5D Hamiltonian for the T-R motions of the guest diatomic molecule is[31]

$$H^{5D} = -\frac{\hbar^2}{2m}\left(\frac{\partial^2}{\partial x^2} + \frac{\partial^2}{\partial y^2} + \frac{\partial^2}{\partial z^2}\right) + B\mathbf{j}^2 + V(x, y, z, \theta, \phi),$$
(1)

where m is the mass of the guest molecule, while B and $\mathbf{j}^2$ are the rotational constant and angular momentum operator, respectively, of the diatomic. $V(x, y, z, \theta, \phi)$ is the 5D PES describing the intermolecular interaction between H$_2$ and MOF-5. For the matrix representation of H^{5D}, the 3D direct-product discrete variable representation (DVR) (Ref. 59) basis in the x, y, z coordinates is combined with the modified (real) spherical harmonics $\overline{Y}_{jm}(\theta, \phi)$ for the angular θ and ϕ

coordinates.[42,57] The resulting 5D direct-product basis is contracted, reduced drastically in size by the procedure described in Ref. 42, with no loss of accuracy. Diagonalization of the matrix of H^{5D} formed in this contracted basis yields the fully coupled 5D T-R energy levels and wave functions of H_2 adsorbed in MOF-5.

B. Fixed-site quantum 2D calculation of the hindered-rotor eigenstates

The 2D rotational energy levels and wave functions of H_2 bound to each of the four principal binding sites of MOF-5 (Refs. 20 and 55) were calculated using the hindered-rotor Hamiltonian denoted H^{2D}, the purely rotational component of the 5D T-R Hamiltonian H^{5D} in Eq. (1),

$$H^{2D} = B\mathbf{j}^2 + V(\theta, \phi), \tag{2}$$

where B and $\mathbf{j}^2$ have the same meaning as in Eq. (1). $V(\theta, \phi)$ is the 2D PES for the rotation of the H_2 molecule with its c.m. fixed, obtained in a manner described later in the paper. The rotational eigenvalues and eigenvectors of H^{2D} are determined by its diagonalization in the angular basis $\{\overline{Y}_{jm}(\theta, \phi)\}$. It should be kept in mind that these 2D calculations, while much faster than those for the full T-R Hamiltonian H^{5D} in Eq. (1), leave out entirely the translational DOFs of H_2 and the T-R coupling. Consequently, their accuracy is uncertain, semiquantitative at best.

C. Potential energy surfaces

1. The five-dimensional potential energy surface

The 5D PES describing the interaction between H_2 and MOF-5 is represented by the analytical potential energy function developed by Belof *et al.*,[7,54] which will be referred to as PES1. The functional form of this potential is simple; it is a sum of Lennard-Jones 6-12 potentials representing the repulsive and van der Waals interactions between H_2 and the framework, and the electrostatic interactions among the point partial charges assigned to each atom in the system.[7,60] This potential function in general accounts also for the effects of many body polarization (induction).[60] However since MOF-5, unlike some other MOFs,[48] does not have exposed metal sites, the contribution of the many-body polarization (*via* the Thole-Applequist model[61–63]) is small and was not included in H_2@MOF-5 PES.[7]

The binding sites of the H_2@MOF-5 system were identified by location of the energy minima using a simulated annealing Monte Carlo process over PES1. The simulated annealing process took the single H_2 (in the MOF) from a high temperature of 5000 K down to 5.0 K over 10 000 000 Monte Carlo steps. To ensure that all binding sites, not just the global minimum, were located without bias, the starting coordinates of H_2 and random number generator seed were initialized over a grid of 250 points within MOF-5 and the simulated annealing calculations for all 250 starting configurations were then run in parallel. This procedure yielded all of the known binding sites in MOF-5 (α, β, δ, γ and ϵ), with no new sites revealed beyond these. Following previ-
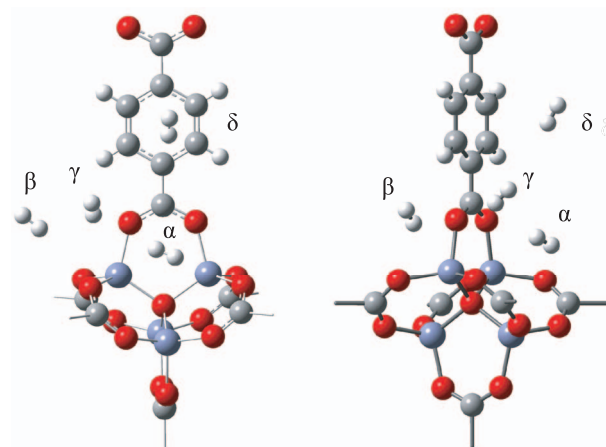

FIG. 1. Two views of the positions of four binding sites of H_2 in MOF-5 as determined by simulated annealing on PES1. Atom colors: H white, O red, C gray, Zn purple.

ous experimental[19,20] and computational work,[8,64–67] here we will consider four binding sites of H_2; those corresponding to the potential minima on PES1 are shown in Fig. 1. Three sites, designated as α, β, and γ, respectively,[20,55] are associated with the $Zn_4O(CO_2)_6$ unit, a node in the cubic array of MOF-5, while the fourth (δ-site[20,55]) is above the face of the phenylene linker.

PES1 is calculated for H_2 interacting with the entire unit cell of MOF-5. Figure 2 displays the 3D isosurface representation of the 5D PES1 in the vicinity of the $Zn_4O(CO_2)_6$ unit; it is obtained by minimizing the H_2-MOF interaction with respect to the two angular coordinates of H_2 at every position of its center of mass. Since the phenylene linkers are not included for reasons of clarity, only the α-, β-, and γ-sites are visible in Fig. 2. It is evident that the PES has a very complex shape. The potential minimum corresponding to the α-site lies in the pocket above the central O atom of the O-centered Zn_4 tetrahedron, equidistant from the three carboxylates. The α-site is trigonally surrounded by the three minima associated with the γ-sites, each located above the edge of a ZnO_4

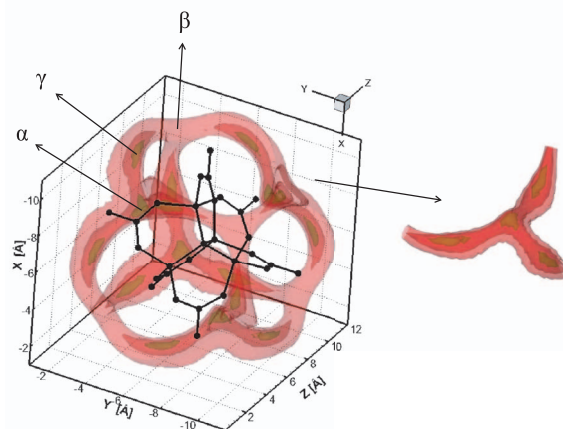FIG. 2. 3D isosurfaces at −62, −56, and −44 meV for the 5D PES1 of H_2 around a MOF-5 fragment. The isosurfaces are obtained by minimizing the H_2-MOF interaction with respect to the two angular coordinates of H_2 at every position of its center of mass.

tetrahedron. The γ-sites around the neighboring α-sites are interconnected *via* the potential minimum identified as the β-site, above the face of a ZnO_4 tetrahedron. There are four α-sites, four β-sites, and twelve γ-sites per $Zn_4O(CO_2)_6$ unit (and six δ-sites on the linkers). The energetics of these binding sites and the (low) barrier heights separating them are discussed later.

2. The two-dimensional rotational potential energy surfaces

For each of the four H_2 binding sites considered, α, β, γ, and δ, two types of 2D rotational PESs were calculated. One set of 2D PESs was obtained from the (5D) PES1 of Belof *et al.*,[7,54] by fixing the c.m. of H_2 at the coordinates of the potential minima with which the four binding sites are associated. We will refer to these four PESs as 2D PES1, to distinguish them from the PES1 above in 5D.

The second set of 2D rotational PESs was computed *ab initio* for H_2 c.m. fixed at the four binding sites which were located using the second-order Møller-Plesset (MP2) perturbation theory with the def2-TZVP basis set of Ahlrichs *et al.*[68,69] In these calculations, two model fragments by Sillar *et al.*[8] were employed, a benzoate model $OZn_4(CO_2Ph)_6$ for the α-site, β-site and γ-site, and the so-called linker model, consisting of the two formate models $OZn_4(CO_2H)_6$ connected by a benzene ring, for the δ-site. It has been shown that these models yield the same binding energy as the full periodic structure.[8] MP2 calculations were performed with the ricc2 module[70–72] of the TURBOMOLE V5.10 program package.[73] A frozen-core approximation and the resolution of identity approximation, also known as density fitting,[74] were employed in these calculations. Binding sites with the adsorbed hydrogen molecules obtained this way are shown in Ref. 8 and will be compared with the ones shown in Fig. 1 later in the text. Each of the four 2D *ab initio* PESs was calculated on a 13×13 grid (symmetrically equivalent points included) with $15°$ increments starting from $\theta = 0°$ and $\phi = 0°$. The data were, as needed, interpolated using the triangulation method.[75] These *ab initio* 2D PESs are designated as 2D PES2.

D. Computational details

In the quantum 5D calculations of the T-R eigenstates of H_2 on PES1, the dimensions of the 1D DVRs[42] were $N_x = N_y = N_z = 35$ for the Cartesian coordinates x, y, and z, respectively, and were distributed over the range $-8.0 \leq x \leq -0.5$ Å, $-8.0 \leq y \leq -0.5$ Å, and $4.4 \leq z \leq 12.4$ Å. The angular basis $|jm\rangle$ included functions up to $j_{max} = 5$, which resulted in an angular basis of 36 $\bar{Y}_{j,m}(\theta, \phi)$ functions. The energy cutoff for the intermediate 3D eigenvectors was set to 50 meV. These parameters resulted in a final full Hamiltonian matrix of dimension $N = 1800$, which is much less than $N = 1\,543\,500$, the dimension of the Hamiltonian matrix in the uncontracted basis with $j_{max} = 5$. All the basis set parameters were tested extensively for convergence. The calculated quantum 5D T-R energy levels up to 30 meV are converged to five significant figures.

The 2D rotational energy levels for the H_2 molecule in the four binding sites α, β, γ, and δ, on the 2D PES1 and 2D PES2 computed for each site, were calculated using the angular basis $|jm\rangle$ with the j up to 7, which led to the basis of 64 $\bar{Y}_{j,m}(\theta, \phi)$ functions. The rotational constant of the H_2 molecule was taken to be $B_{H_2} = 59.3$ cm$^{-1} = 7.35$ meV.

III. RESULTS AND DISCUSSION

A. Binding sites for H_2 in MOF-5: Comparison of theory and experiment

Experimental information on structural details of the binding sites of hydrogen in MOFs and related porous systems is extremely difficult to obtain by diffraction methods, and only indirect information can be deduced from spectroscopic data. The adsorbed hydrogen molecule cannot be reliably located by X-ray diffraction on account of its weak scattering of X-rays and minimal contrast to many of the other atoms in the system. Single-crystal neutron diffraction with its great sensitivity to hydrogen, on the other hand, would be the method of choice for this purpose, were if not for inadequate size of single crystals of MOFs. Only one such experiment has been carried out to date on H_2 in MOF-5.[11] Neutron powder diffraction has also been used,[10] although in this case it is important that most, if not all the H atoms that are part of the framework also be deuterated, and that the results for the hydrogen binding sites do not have the same level of accuracy (most notably the thermal parameters) as would be possible for single-crystal neutron diffraction. INS measurements have been used in a number of cases[20,23,76–78] to obtain some details on binding sites and their relative populations, and it is the interpretation of these data that would benefit enormously from direct computational analysis and support, as we will show in the remaining section.

It has, however, been possible to use single-crystal X-ray diffraction from N_2 and Ar absorbed in MOF-5 to identify in great detail a total of five primary binding sites.[55] Three of these are located on the inorganic cluster (α-site, β-site, and γ-site) and two of them on the phenylene link (δ-site and ϵ-site). It was also concluded that the relative binding energies decrease in the order: α-site $\gg \beta$-site $> \gamma$-site $> \delta$-site $\approx \epsilon$-site, but it was emphasized that the occupation of γ-site was preferred over that of the β-site at low temperatures because of the greater multiplicity of the former and the resultant increase in the packing efficiency at the cluster surface.[55]

A large number of quantum chemistry calculations of adsorption energies for H_2 in MOF-5 at different levels of theory have also been reported, both DFT studies using either periodic or cluster models and different functionals[8,10,65,79,80] as well as the more expensive MP2 calculations on clusters.[8,64–67] The relative stability and binding energies can be seen to depend strongly on the level of calculation used. Nonetheless, most studies identify the α-site as the minimum-energy site for the hydrogen molecule.[8,10,65,67]

We considered four hydrogen binding sites in our calculations for PES1 (Fig. 1) and at the counterpoise-corrected (CP-corrected) MP2/common board sets (CBS(D,T))//MP2/def2-TZVP level of theory (2D PES2),[8]

namely, the α-, β-, and γ-sites around the inorganic cluster and one site on the phenylene link, the δ-site. The geometric parameters for H_2 in the primary binding site (α) on the 2D PES2 and PES1 may be compared to the experimental values obtained from single crystal neutron diffraction.[11] From the latter (supplementary material in Ref. [11]) it can be deduced that the H_2 c.m. is at the distance of 3.95 Å from the central oxygen. On the other hand, in the α-site in PES1 the c.m. of H_2 is 3.72 Å away from the central oxygen atom of the cluster, while the CP-corrected MP2/CBS(D,T)//MP2/def2-TZVP fully optimized cluster places the H_2 c.m. 3.6 Å from the central oxygen. It should be kept in mind that these theoretical results are equilibrium values, whereas the experiment measures vibrationally averaged distances, which are always greater due to the anharmonicity of the PES. Indeed, as discussed later, the quantum 5D calculations on PES1 give for the α-site the expectation value of the distance of the H_2 c.m. to the central oxygen of the OZn_4 cluster which is 0.5 Å greater than its equilibrium distance.

The single-crystal neutron diffraction work[11] reports structural information for only one additional binding site, namely, the distance of the c.m. of H_2 in the β-site of 3.64 Å from the nearest Zn atom. The equilibrium values calculated on PES1, 3.61 Å, and 2D PES2, 3.68 Å, are in excellent agreement with the result from the diffraction experiment.

On PES1 the α-site is the global minimum with the energy of -66.6 meV. The three other sites are the γ-site at -65.5 meV, only 1.1 meV higher than the α-site, β-site with an energy of -53.8 meV and the linker site (δ-site) located above the benzene ring with the energy of -37.8 meV. The binding energies determined for the benzoate model at the CP-corrected MP2/CBS(D,T)//MP2/def2-TZVP level of theory[8] also predict that the α-site is the most stable with the binding energy of -82.9 meV. The γ-site lies 29.0 meV higher (compared to 1.1 meV on PES1), at -53.9 meV, followed by the δ-site with the well depth of -52.9 meV, and the β-site with the weakest binding energy of -47.7 meV. Previous MP2 and DFT calculations on clusters using HCTH, PW91, and PBE functionals,[67,79] as well as periodic DFT calculations with the van der Waals density functional (vdW-DF) approach,[81] have also found large differences in binding energies between the α-site and the γ-site, ranging from 12.5 to 16.4 meV,[79] to 20.7 meV,[67] and 34.2 meV.[81] We therefore conclude that in all likelihood PES1 underestimates the difference in binding energy between the α- and γ-sites, while that obtained for the 2D PES2 is in line with the experimentally deduced relative stabilities of these two binding sites.[55]

Another conspicuous feature of PES1 is the low translational barrier between the neighboring α- and γ-sites, less than 11 meV. This is shown more clearly in Fig. 3 which presents a 2D cut through the 3D isosurfaces (Fig. 2) connecting the α-site with one of the three neighboring γ-sites. It is evident that the H_2 molecule is generally not localized in an α-site, but can readily access the three γ-sites in the immediate vicinity already at low translational excitation. As a consequence, the excited 5D T-R energy levels for H_2 could not be converged for an isolated α-well. Instead, the 5D T-R bound-state problem had to be solved for a much larger
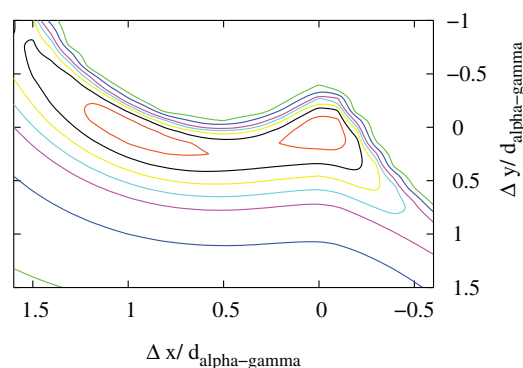

FIG. 3. A 2D cut through a 5D potential of H_2 in MOF-5 (shown in Fig. 2) connecting the α-site at (0,0) and one of the γ-sites at (1,0); $d_{alpha-gamma} = 3.0$ Å. Isosurfaces are shown at every 6 meV, starting from -62 meV, and are obtained by minimizing the H_2-MOF interaction with respect to the two angular coordinates of H_2 at every position of its center of mass.

region of space which includes the α-site together with the three neighboring γ-sites, as presented on the right side of Fig. 2. The rotational excitations from these quantum 5D calculations can be compared with the 2D rotational energy levels computed for the case in which the c.m. of the hydrogen molecule is fixed in the α-site or γ-sites, respectively.

B. 2D rotational energy levels of H_2 at different binding sites

The 2D rotational energy levels of H_2 at all four binding sites, calculated on both 2D PES1 and 2D PES2, are presented in Tables I and II, respectively. The rotational levels for the α-site computed on the two PESs agree remarkably well. Both PESs predict that the threefold degeneracy of the $j = 1$ level is lifted completely due to the angular anisotropy of the interaction potential at the α-site. The $j = 1$ level is split into three states that span the energy range of 10.8–22.6 meV for 2D PES1 and 10.1–22.8 meV for 2D PES2. One of the three $j = 1$ sublevels is close to the energy of the $j = 1$ free rotor level for H_2 in the gas phase (14.7 meV) while the other two are ≈ 4 meV below and ≈ 8 meV above this level, respectively, resulting in the total splitting for the $j = 1$ triplet of 11.8 meV on the 2D PES1, and 12.7 meV on the 2D PES2. A

TABLE I. Rotational energy levels of H_2 at different binding sites in MOF-5 from quantum 2D calculations on 2D PES1. The energies are given relative to the $j = 0$ level which is 10.8, 19.2, 1.0, and 11.3 meV, respectively, above the minima corresponding to the α-, γ-, δ-, and β-sites.

n	α-site ΔE (meV)	γ-site ΔE (meV)	δ-site ΔE (meV)	β-site ΔE (meV)	
1	0.0	0.0	0.0	0.0	$j = 0$
2	10.8	7.5	14.4	10.1	
3	13.3	20.2	14.9	17.5	$j = 1$
4	22.6	21.1	14.9	18.0	
5	40.1	42.0	43.9	42.0	
6	40.1	42.4	44.0	42.7	
7	46.8	43.2	44.0	43.0	$j = 2$
8	48.6	52.3	44.4	48.4	
9	51.6	52.3	44.4	48.5	

TABLE II. Rotational energy levels of H_2 at different binding sites in MOF-5 from quantum 2D calculations on the 2D PES2 (MP2/CBS(D,T)//MP2/def2-TZVP level). The energies are given relative to the $j = 0$ level which is 12.6, 8.4, 4.4, and 8.7 meV, respectively, above the minima corresponding to the α-, γ-, δ-, and β-sites.

| n	α-site ΔE (meV)	γ-site ΔE (meV)	δ-site ΔE (meV)	β-site ΔE (meV)	
1	0.0	0.0	0.0	0.0	$j = 0$
2	10.1	11.6	12.8	11.3	
3	14.1	13.8	15.1	15.6	$j = 1$
4	22.8	20.1	16.4	18.1	
5	40.2	41.1	42.9	41.9	
6	40.2	41.2	42.9	42.4	
7	46.3	45.7	43.8	43.9	$j = 2$
8	49.2	47.3	45.7	47.0	
9	51.9	48.7	45.8	47.6	

FIG. 4. Rotational 2D $V(\theta, \phi)$ potentials projected on a sphere traced by hydrogen molecule rotating with their center of mass fixed: (a) 2D PES1 α-site, (b) 2D PES2 α-site, (c) 2D PES1 γ-site, and (d) 2D PES2 γ-site. Energies in meV are given relative to the energy of the potential minima of the corresponding binding site.

similar splitting was observed in the case of hydrogen at the Zn site in MOF-74 where the three corresponding $j = 1$ transitions are calculated to be in the range of 10.6–21.6 meV.[30]

This similarity extends also to the $j = 2$ quintuplet for H_2 in the α-site, which is split into five distinct components lying between 40.1 and 51.6 meV on 2D PES1 and 40.2 and 51.9 meV on 2D PES2. On both potentials the splitting pattern is as follows: the "central" state is close to the energy of the (fivefold degenerate) $j = 2$ level in the gas phase (44.1 meV), while the four remaining states are grouped in two pairs, one pair energetically above and the other below the central state. It is interesting to note that the same splitting pattern was found in the calculations of the $j = 0 \rightarrow j = 2$ transition of H_2 in the small cage of the sII clathrate hydrate,[32] and also for H_2 on the amorphous ice surface,[82] although these environments have little in common with the α-site in MOF-5.

The rotational energy levels for H_2 in the γ-site calculated on 2D PES1 and 2D PES2 differ substantially, unlike those computed on these two PESs for the α-site. This is not surprising, since already a visual comparison of the two 2D rotational PESs at the γ-site (Fig. 4) reveals their marked differences, in contrast to the 2D PES1 and 2D PES2 for the α-site which are very similar. The angular anisotropy of the 2D PES1 at the γ-site is considerably larger than on the 2D PES2. This is evident from the greater splitting of the $j = 1$ triplet on the 2D PES1, 13.6 meV, as compared to 8.5 meV for 2D PES2. As a result, on the 2D PES1 the lowest energy sublevel of the $j = 1$ triplet is pushed further down from the gas-phase value of 14.7 meV, to 7.5 meV, than on the 2D PES2, where it lies at 11.6 meV. Weaker angular anisotropy of the 2D PES2 in the γ-site is reflected also in the smaller splitting of the $j = 2$ quintuplet, 7.6 meV, relative to 10.3 meV calculated for the 2D PES1.

2D PES1 exhibits greater angular anisotropy than 2D PES2 at the β-site as well, apparent from the larger splittings of both the $j = 1$ triplet (7.9 vs. 6.8 meV) and the $j = 2$ quintuplet (6.5 vs. 5.7 meV).

At the δ-site which is located on the phenylene link, the splittings of the $j = 1$ and $j = 2$ multiplets calculated on both 2D PES1 and 2D PES2 are much smaller than at the α-, β-, and γ-sites around the inorganic cluster. This indicates that,
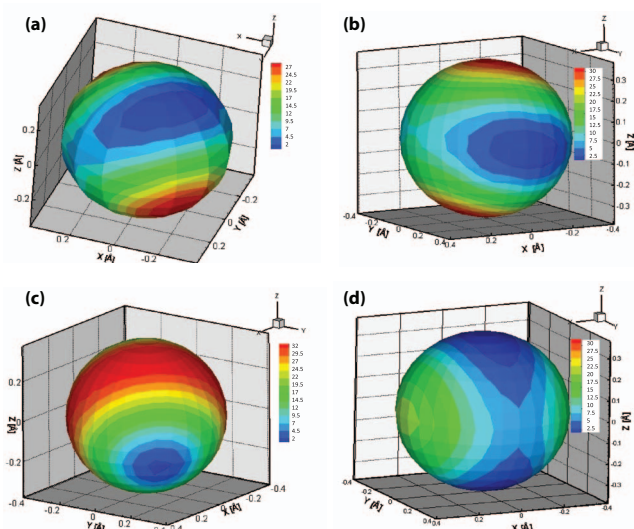
as expected, the angular anisotropy of the interaction of H_2 with the organic linker is much weaker than with the inorganic node. Interestingly, the rotational multiplet splittings at the δ-site, and hence the angular anisotropy, are much smaller on the 2D PES1, 0.5 meV for $j = 1$ and $j = 2$, than on 2D PES2, 3.6 meV for $j = 1$ and 2.9 meV for $j = 2$.

C. 5D translation-rotation energy levels

The T-R energy levels from the quantum 5D calculations of the H_2 molecule bound in the region of PES1 encompassing an α-site and three γ-sites surrounding it are given in Table III. By projecting a 5D T-R eigenstate on the rotational basis, we can determine the contribution of each rotational basis function to that eigenstate and determine whether they are rotationally excited or not.[31] Table III lists contributions from the $j = 0$ and $j = 1$ rotational basis functions to each eigenstate. The translational excitations are visualized with the help of the 3D reduced probability densities (RPDs) $\rho_n(x, y, z)$ in Cartesian coordinates, defined as

$$\rho_n(x, y, z) = \int \psi_n^*(x, y, z, \theta, \phi) \psi_n(x, y, z, \theta, \phi) \sin\theta \, d\theta \, d\phi,$$
(3)

where $\psi_n(x, y, z, \theta, \phi)$ is the 5D T-R wave function of the H_2 molecule inside MOF-5. The 3D RPDs of some of the 5D T-R eigenstates of H_2 which are sufficiently regular are displayed in Figs. 5 and 6. The appearance and the nodal patterns of these RPDs are very intricate, reflecting the complex topography and symmetry of the part of the 5D PES which they probe. As a result, the task of understanding the computed T-R energy levels structure and finding the quantum numbers appropriate for the assignment of the excited T-R states of H_2 in MOF-5 is far more difficult than in the case of H_2 inside the cages of sII clathrate hydrate,[31–33] fullerenes,[16,34,36–38] and for some other single- and double-well systems.[58,83,84] The mod-

TABLE III. T-R energy levels of H_2 from the quantum 5D calculations on the region of PES1 encompassing the α-site and the three neighboring γ-sites. The excitation energies ΔE (in meV) are given relative to the ground-state energy $E_0 = -39.6$ meV. The columns labeled $j = 0$ and $j = 1$ represent the contributions of the corresponding rotational basis functions to the 5D T-R wave functions.[31]

n	ΔE	$j = 0$	$j = 1$
1	0.0	**0.98**	0.00
2	5.28	**0.98**	0.00
3	5.28	**0.99**	0.00
4	5.56	**0.99**	0.00
5	6.91	**0.99**	0.00
6	6.91	**0.99**	0.00
7	7.53	**0.99**	0.00
8	9.59	**0.98**	0.00
9	9.59	**0.98**	0.00
10	9.89	**0.98**	0.00
11	11.48	**0.99**	0.00
12	11.50	**0.99**	0.00
13	12.54	**0.98**	0.00
14	12.58	**0.98**	0.00
15	12.58	**0.98**	0.00
16	12.61	**0.99**	0.00
17	12.92	0.00	**0.99**
18	12.94	0.00	**0.99**
...			
36	16.69	0.00	**0.99**

FIG. 6. 3D isosurfaces of the reduced probability densities in the Cartesian coordinates of several 5D T-R states of H_2 in Table III with two or more quanta excitation in the translational degrees of freedom and $j = 0$. The isosurfaces are drawn at 15% of the maximum density.

els of 2D and 3D isotropic harmonic oscillator, which proved surprisingly useful in assigning the T-R eigenstates of H_2 (and CH_4[58]) in clathrate hydrate cages,[32,33] and fullerenes,[34–36] were of no help in this case. The level scheme of the translational excitations will, however, be discussed in more detail below.

The excitation energies (ΔE) in Table III are given relative to 5D T-R ground state energy of H_2, -39.6 meV. Since
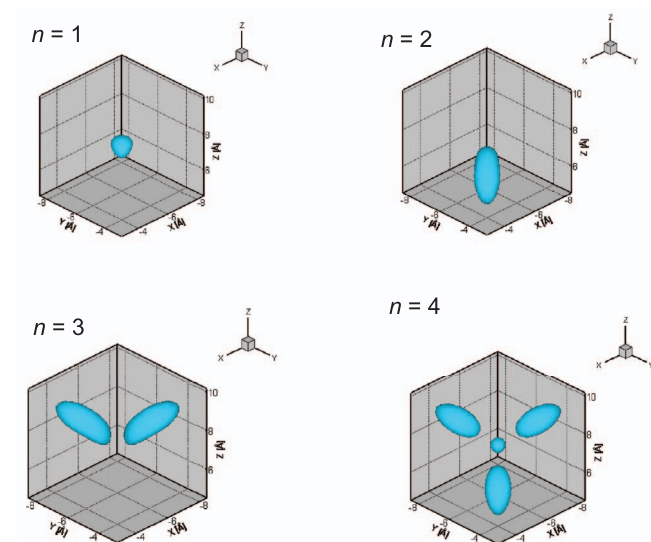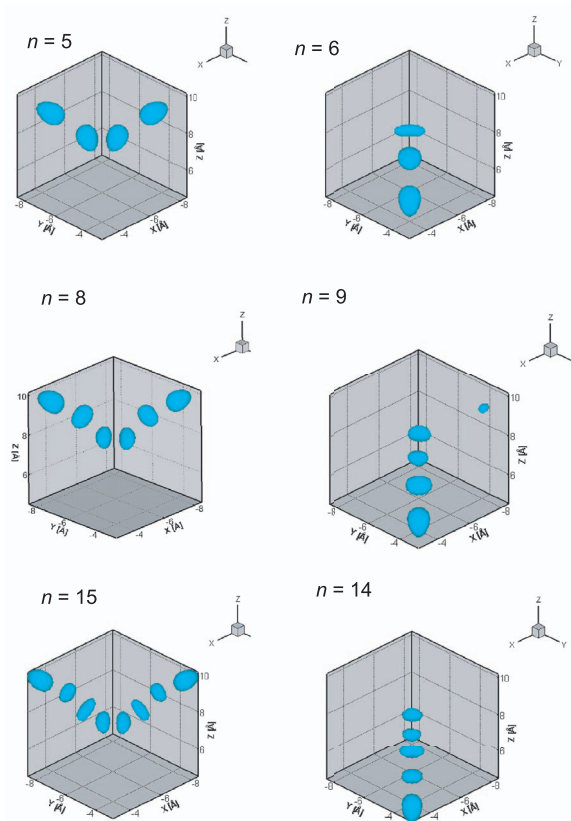

FIG. 5. 3D isosurfaces of the reduced probability densities in the Cartesian coordinates of lowest four 5D T-R states of H_2 in Table III ($j = 0$). The isosurfaces are drawn at 15% of the maximum density.

the global minimum of PES1 is at -66.6 meV, the zero-point energy (ZPE) of the coupled T-R motions is therefore equal to 27.0 meV. This value is comparable to some previously obtained ZPEs associated with the H_2 c.m. translational motion in MOF-5. A simple isotropic 3D harmonic oscillator model for the c.m. translational frequency of 10.4 meV measured by the diffuse reflectance IR spectroscopy[53] gives the translational ZPE of 15.5 meV, while Sillar *et al.*[8] and Kong *et al.*[81] both predict values of 21 meV. When the later value is combined with the 2D rotational results of 5 meV (Ref. 81) and 12.6 meV (2D PES2 this work) total zero point energies of 26 meV and 33 meV are obtained. We can thus conclude that the total zero point energy is in the range of 30 ± 3 meV.

Sillar *et al.*[8] have pointed to the important role of vibrational-rotational zero-point energies for calculated heats of adsorption. Using the thermal contribution to the heat of adsorption at 77 K from Ref. 8 (3 vibrational degrees of freedom) of -11.4 meV, we arrive at a total difference between the heat of adsorption and the adsorption energy (minimum on the potential energy surface) of 18.7 ± 3 meV for the α-site. Consistent with this result is the difference of 22.0 meV between the initial isosteric heat of adsorption obtained by Belof *et al.*[7] using grand canonical Monte Carlo simulations for PES1 and a semiclassical correction term that takes quantum effects on nuclear motions into account (44.6 meV) and the binding energy for PES1 (66.6 meV).

This difference can further be used to derive observed adsorption energies for testing different quantum chemical methods and force fields. From the heat of adsorption of 68.4 meV (Ref. 21) and 60.1–70.5 meV (Ref. 85) observed for low hydrogen loadings at 77 K we infer adsorption energies of 87.1 ± 3 and 83.9 ± 8 meV. The MP2 result for the binding energy (82.9 meV) (Ref. 8) is in excellent agreement, whereas the vdW-DF result (115 meV) (Ref. 81) and the result for PES1 (66.6 meV, this work) are outside the relevant range.

The lowest sixteen T-R energy levels ($n = 1$–16) listed in Table III are purely translational excitations, given that the contribution from the dominant $j = 0$ rotational basis function is 0.98 or greater. The first three excited 5D T-R energy levels $n = 2$–4 appear as a degenerate pair of states $n = 2$, 3 at 5.3 meV and a distinct one ($n = 4$) at 5.6 meV, respectively. As shown by Fig. 5, while the ground-state RPD is localized in the (global) potential minimum of the α-site, the RPDs of first three translationally excited states extend to the three local minima corresponding to the neighboring γ-sites. Comparison of the RPDs of the higher energy T-R eigenstates displayed in Fig. 6 with those in Fig. 5 leads one to conclude that the degenerate states $n = 5$ and $n = 6$, $n = 8$ and $n = 9$, and $n = 14$ and $n = 15$ given in Table III represent successively higher excitations of the degenerate pair $n = 2$, 3. In the same vein, one can infer that the non-degenerate levels $n = 7, 10, 13$ represent higher excitations of the state $n = 4$, while the levels $n = 11, 12$ and 16 correspond to the combination excitations of states $n = 2$–4.

The states $n = 17, 18$, and 36 in Table III are the lowest energy purely rotational excitations of H_2 in the ground translational state, with the contribution of the dominant $j = 1$ rotational basis function equal to 0.99. They constitute the three components of the $j = 1$ triplet whose degeneracy has been lifted by the angular anisotropy of the binding site. Two of them, $n = 17, 18$ at 12.92 and 12.94 meV, respectively, have energies below that of the $j = 1$ level in the gas phase, 14.7 meV, while the third, $n = 36$, has its energy pushed higher, to 16.7 meV. Thus, the $j = 1$ triplet is split by 3.8 meV. We have to point out that the three $j = 1$ levels should, in principle, correspond to the two states having $m = -1, 1$ and to one state having $m = 0$. However, all three basis functions with the same j but different m quantum number contribute significantly to $n = 17, 18$, and 36 states (their sum is equal to 0.99, Table III) so that a quantum number m could not be assigned to any of the 5D T-R eigenstates.

The splitting of the $j = 1$ triplet from the quantum 5D T-R energy level calculations, 3.8 meV, is much smaller than the corresponding $j = 1$ splittings obtained by solving the purely rotational quantum 2D problem of H_2 c.m. fixed at the α-site, 11.8 meV on the 2D PES1 (Table I) and 12.7 meV on the 2D PES2 (Table II). A partial explanation for this difference can be found by comparing the positions of the hydrogen molecule in the two types of dynamical calculations. Analysis of the quantum 5D ground-state wave function for H_2 in the α-site basin gives the vibrationally averaged distance of 4.24 Å from the H_2 c.m. to the central O atom of the inorganic cluster, which is 0.5 Å larger than the equilibrium value of 3.72 Å (PES1) for the minimum-energy geometry at which the H_2 c.m. is fixed in quantum 2D rotational calculation. One

expects that, as a result of the greater distance from the OZn_4 cluster, the angular anisotropy of the interaction experienced by the H_2 molecule in the fully coupled quantum 5D calculations is weaker, giving rise to a smaller calculated splitting of the $j = 1$ triplet. In order to test this conjecture, the quantum 2D rotational calculations were repeated on the 2D PES1 for the H_2 c.m. fixed 4.24 Å from the center of the inorganic cluster. They yielded the $j = 1$ triplet splitting of 4.6 meV, close to 3.8 meV obtained in the quantum 5D calculations; the energies of the sublevels obtained in this way, ranging from 13.3 to 17.9 meV, also compare favorably with those from the quantum 5D calculations, 12.9 to 16.7 meV (Table III). All this demonstrates the necessity to include the T-R coupling in theoretical treatments aiming for quantitative accuracy, and the limitations of the reduced-dimension approaches where it is neglected.

D. Comparison with the experiment

The T-R transition energies from the fully coupled quantum 5D calculations on PES1 are compared with the experimental INS spectrum in Fig. 7, where the calculated transitions are shown as a stick diagram. Most of the experimental INS spectra were previously reported.[19, 20] These data were collected at 10 K on the inverse geometry quasielastic neutron scattering (QENS) spectrometer at the Intense Pulsed Neutron Source of Argonne National Laboratory. Adsorption of a given amount of hydrogen was carried out at 77 K, followed by a period of equilibration and gradual cooling to 10 K for the measurement. The experimental INS spectrum for the lowest loading of four H_2 molecules per formula unit (*i.e.,* one H_2 per cluster) shows peaks at 10.3, 12.1, 19.2, and 22.4 meV with two additional low-intensity peaks at 24.4 and 27.5 meV, which can all be attributed the T-R excitations of the adsorbed H_2. This spectrum should correspond to full occu-
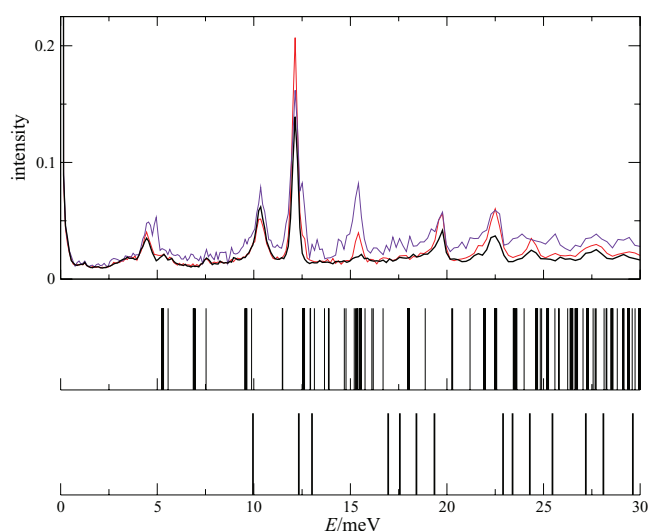

FIG. 7. Experimental INS spectrum (top)[19, 20] for different loadings of H_2 in MOF-5 (black: 4 H_2, red: 8 H_2, and violet: 24 H_2 per formula unit), in comparison to the quantum 5D T-R energy levels calculated for a single H_2 in the basin encompassing the α- and γ-sites (middle), and for H_2 moving within the α-site and the neighboring γ-sites occupied by static H_2 molecules (bottom).

pation of the α-sites, provided that in the process of slow cool of the sample from 77 K all hydrogen molecules indeed find their way to the lowest energy binding site. The peak near 4.5 meV is actually an excitation of the torsional mode of the BDC linkers in the MOF-5 frame, since it also appears in the INS spectrum of MOF-5 in the absence of adsorbed H_2.

The lowest lying transitions obtained in the 5D T-R calculation in the range of 5–8 meV (Table III) have no obvious counterparts in the INS spectrum. While it is, in principle, possible that these excitations have vanishing intensities in the INS spectrum, this is not likely to be the case. Any low frequency mode involving hydrogen would have large vibrational amplitudes, and hence significant INS intensity. We therefore attribute the low energies of these transitions to the nature of the PES1 used for this calculation, which results in an underestimate of the energies of the lowest translational excitations. The features of PES1 described earlier, namely, that the well depth of its γ-site is almost as deep as that for the α-site, and that the barrier between the two sites is low, produce an extensive delocalization of the wave function and large-amplitude translational excitations with very low frequencies. This delocalization, however, is not in agreement with experimental results, and hence points to deficiencies in PES1. This will be discussed in more detail below.

The peak at 10.3 meV in the experimental INS spectrum in Fig. 7 is very close in energy to the transition observed at 10.4 meV in the diffuse reflectance IR spectra of H_2 in MOF-5,[53] which was shown to be a translational excitation of H_2 in the α-site. It is therefore reasonable to assume that the peak in the INS spectrum has the same origin. As Table III shows, quite a few purely translational ($j = 0$) excitations lie in the energy range between 9.6 and 12.6 cm^{-1}, and are therefore plausible candidates for the 10.4 meV peak.

By far the strongest peak in the measured INS spectrum appears at 12.1 meV, which is energetically close to the two nearly degenerate components of the $j = 1$ triplet at 12.9 cm^{-1} in Table III. Consequently, the most likely assignment of this peak is the purely rotational excitation of H_2 in the α-site. One is then tempted to assign the peak observed at 19.2 cm^{-1} to the highest energy component of the $j = 1$ triplet calculated to lie at 16.7 cm^{-1} (Table III).

At higher H_2 loadings the γ-site become occupied as well, presenting theory with a most challenging dynamical problem of at least four interacting hydrogen molecules, one in the α-site and three in the neighboring γ-sites. This system has twenty DOFs, and a rigorous eigenstate-resolved treatment of its fully coupled quantum T-R dynamics is not feasible at the present time. Therefore, as a first approximation we performed the quantum 5D calculations of the T-R eigenstates of H_2 in the α-site, with each of the three surrounding γ-sites occupied by one H_2 held fixed at the minimum-energy geometry. The H_2 interaction with MOF-5 was represented by the 5D PES1, and the H_2–H_2 interactions were taken into account as described in Ref. 54. The resulting 5D PES, shown in Fig. 8, is much more localized, as the H_2 in the α-site can no longer easily move to the neighboring γ-sites.

The lower-lying 5D T-R energy levels calculated on this PES are given in Table IV, together with the root mean
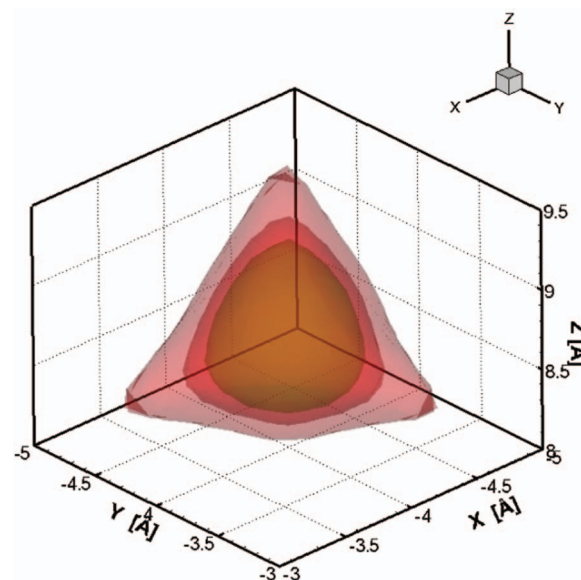

FIG. 8. 3D isosurfaces at -62, -50, and -31 meV, respectively, of the 5D intermolecular PES of H_2 in the α-site of MOF-5, with each of the three neighboring γ-sites occupied by an H_2 molecule. The isosurfaces are obtained by minimizing the H_2-MOF interaction with respect to the two angular coordinates of H_2 at every position of its center of mass.

squared (rms) amplitudes Δx, Δy, and Δz which can serve as a measure of the wave function delocalization in the $x-$, $y-$, and $z-$ directions, respectively.[31] The lowest energy translational ($j = 0$) excitation now lies at 10.0 meV, while the three components of the $j = 1$ rotational level (in the ground translational state) have the energies of 12.3, 13.0, and 19.4 meV, respectively, so that the overall $j = 1$ triplet splitting is 7.1 meV. The energy levels $n = 9$, 10, and 14, at 22.9, 23.4, and 28.1 meV, respectively, are the combination of the translational excitation ($n = 2$) at 10.0 meV with the three $j = 1$ sublevels $n = 3$, 4, and 8, respectively. It is evident

TABLE IV. T-R energy levels of H_2 in an α-site of MOF-5 with each of the three neighboring γ-sites occupied by an H_2 molecules, from the quantum 5D calculations on PES1. The excitation energies ΔE (in meV) are given relative to the ground-state energy $E_0 = -35.1$ meV. Also shown are the root-mean-square (rms) amplitudes Δx, Δy, Δz in Å. The columns labeled $j = 0$ and $j = 1$ represent the contributions of the corresponding rotational basis functions to the 5D T-R wave functions.[31]

n	ΔE	Δx	Δy	Δz	$j = 0$	$j = 1$
1	0.0	0.27	0.27	0.25	**0.98**	0.00
2	10.0	0.41	0.41	0.35	**0.99**	0.00
3	12.3	0.27	0.27	0.25	0.00	**0.99**
4	13.0	0.27	0.27	0.25	0.00	**0.99**
5	17.0	0.34	0.34	0.47	**0.99**	0.00
6	17.6	0.39	0.39	0.25	**0.98**	0.00
7	18.4	0.49	0.49	0.42	**0.99**	0.00
8	19.4	0.28	0.28	0.26	0.00	**0.99**
9	22.9	0.40	0.40	0.33	0.00	**0.99**
10	23.4	0.40	0.40	0.33	0.00	**0.99**
11	24.3	0.50	0.50	0.32	**0.99**	0.00
12	25.5	0.50	0.50	0.32	**0.99**	0.00
13	27.2	0.53	0.53	0.50	**0.99**	0.00
14	28.1	0.42	0.42	0.37	0.00	**0.99**

from Fig. 7 that these T-R excitations match rather well the bands observed in the INS spectrum for the lowest loading (at 10.3, 12.1, 19.2, 22.4, 24.4, and 27.5 meV), which corresponds to essentially full occupation of the α-sites. This observation suggests again that at very low temperatures (10 K) the actual degree of localization of H_2 in the α-site may be greater than exhibited on the 5D PES1.

Finally, we note that in contrast to the translational excitations, the energies of the components of the $j = 1$ rotational triplet from the quantum 5D calculations on PES1 (Table III) and the modified PES in Fig. 8 (Table IV) are rather similar. The implication is that the purely rotational excitations are much less sensitive to the details of the PESs employed than the translational excitations. This is probably due to the fact that on both PESs the rotationally excited states (with no quanta in translation) are essentially localized in the α-site, unlike the translational excitations, and therefore not particularly sensitive to whether the neighboring γ-sites are unoccupied, as in PES1, or have other H_2 molecules bound to them.

IV. CONCLUSIONS

We have reported the results of the rigorous quantum 5D calculations of the T-R energy levels and wave functions of a single H_2 molecule adsorbed in MOF-5. The quantum dynamics of the translational and rotational motions of H_2 adsorbed in a MOF (assumed to be rigid) was for the first time treated as coupled with full dimensionality in our study. We utilized a recently developed analytical potential energy surface,[7,54] (5D PES1) in these 5D calculations. A purely rotational 2D potential energy surface (2D PES2) was computed *ab initio*[8] with the c.m. of H_2 fixed at each of the four primary binding sites of MOF-5 previously identified.[20,55] Three of these sites, designated as α, β, and γ, are on the $Zn_4O(CO_2)_6$ unit, an inorganic node in the cubic array of MOF-5, while the fourth, the δ-site, is located above the face of the phenylene organic linker. Four additional 2D rotational potential energy surfaces were obtained with 5D PES1, again by placing the c.m. of H_2 at the equilibrium position at each of the four binding sites. We then obtained the purely rotational transitions of H_2 for both rotational potential energy surfaces. We present detailed comparisons between our theoretical results and the available experimental information both with respect to the relative energetics of the binding sites and the excitations of the H_2 molecule bound to them.

Our computational study represents an extremely important step in the effort to expand the atomic level characterization of binding of H_2 in porous materials as the dynamics of the sorbed molecule is far more sensitive to the details of the potential energy surface than equilibrium, or static properties, and this is indeed what we observe in this work. Since the calculation of the 5D quantum dynamical T-R energy levels is exact, the problems we have encountered in obtaining agreement with the experimental results can be traced to inadequacies of the potential energy surfaces we were able to use. It is clear that it is not sufficient to have computational methods account for the bulk properties such as adsorption isotherms (as do both PES1 and PES2), if one wishes to have an accurate picture of the interactions with the host material, as this re-

quires that the potential energy surface describe the H_2–MOF interaction with uniformly high accuracy over a wide range of intermolecular coordinates, which is difficult to achieve for host materials which are chemically as complex as MOFs.

Previous applications of our methodology to systems where the H_2 molecule is constrained to a specific binding site and where the potential energy surface is well established, such as clathrate hydrate cages,[31–33] fullerenes C_{60},[34–37] C_{70},[36,37] and ATOCF[38] have given a rather good account of experimentally observed transitions. In the present case, however, the potential energy surface for H_2 adsorbed in MOF-5 is much more complex than anything we have previously dealt with. The distinctive characteristics of the analytical 5D PES1, for example, is the hierarchy of global and local minima, which are elaborately interconnected by low barriers and thus can give rise to novel features of the quantum T-R dynamics of the adsorbed H_2. The resulting high degree of delocalization of the wave function presents significant computational challenges, since the translational basis has to cover an extended region of the PES encompassing the α-site and the three nearest neighbor γ-sites in order to achieve converged results. Available experimental information, however, clearly shows that only the alpha site is occupied at low temperatures and low loadings, and thereby points to deficiencies in the PES1 which we used for the 5D T-R calculation.

The present study nonetheless constitutes a significant step forward in the detailed atomic-level characterization of the guest–host potential interactions and the quantum dynamics of H_2 adsorbed in MOFs by means of a close interaction between an exact theoretical treatment of the dynamics, a high-level theoretical potential energy surface and spectroscopic results. It demonstrates that theory is rapidly approaching the point where it will be able to extract the full information content of INS and IR spectroscopies of H_2 adsorbed in MOFs with respect to the fine details of the intermolecular PES and the dynamics of guest molecule within. Work is in progress to make the necessary improvements in the potential energy surfaces and to directly simulate the INS spectra of H_2 in MOF-5 using the 5D eigenstates within a more accurate PES.

[1]M. Fichtner, Adv. Eng. Mater **7**, 443 (2005).
[2]L. Schlapbach and A. Züttel, Nature (London) **414**, 353 (2001).
[3]R. E. Morris and P. S. Wheatley, Angew. Chem., Int. Ed. **47**, 4966 (2008).
[4]K. M. Thomas, Catal. Today **120**, 389 (2007).
[5]I. Cabria, M. J. Lopez, and J. A. Alonso, Phys. Rev. B **78**, 205432 (2008).
[6]J. Fu and H. Sun, J. Phys. Chem. C **113**, 21815 (2009).
[7]J. L. Belof, A. C. Stern, and B. Space, J. Phys. Chem. C **113**, 9316 (2009).
[8]K. Sillar, A. Hofmann, and J. Sauer, J. Am. Chem. Soc. **131**, 4143 (2009).
[9]G. L. Squires, *Introduction to the Theory of Thermal Neutron Scattering* (Dover, New York, 1996).
[10]T. Yildirim and M. R. Hartman, Phys. Rev. Lett. **95**, 215504 (2005).
[11]E. C. Spencer, J. A. K. Howard, J. G. McIntyre, J. L. C. Rowsell, and O. M. Yaghi, Chem. Commun. **3**, 278 (2006).
[12]A. J. Ramirez-Cuesta, M. J. Jones, and W. I. F. David, Mater. Today **12**(11) 54 (2009).
[13]G. J. Kearley and M. R. Johnson, Vib. Spectrosc. **53**, 54 (2010).
[14]A. J. Horsewill, K. S. Panesar, S. Rols, M. R. Johnson, Y. Murata, K. Komatsu, S. Mamone, A. Danquigny, F. Cuda, S. Maltsev, M. C. Grossel, M. Carravetta, and M. H. Levitt, Phys. Rev. Lett. **102**, 013001 (2009).
[15]A. J. Horsewill, S. Rols, M. R. Johnson, Y. Murata, M. Murata, K. Komatsu, M. Carravetta, S. Mamone, M. H. Levitt, J. Y. C. Chen, J. A. Johnson, X. Lei, and N. J. Turro, Phys. Rev. B **82**, 081410(R) (2010).
[16]S. Mamone, J. Y. C. Chen, R. Bhattacharyya, M. H. Levitt, R. G. Lawler, A. J. Horsewill, T. Rõõm, Z. Bačić, and N. J. Turro, Coord. Chem. Rev. **255**, 938 (2011).
[17]L. Ulivi, M. Celli, A. Gianassi, A. J. Ramirez-Cuesta, D. J. Bull, and M. Zoppi, Phys. Rev. B **76**, 161401(R) (2007).
[18]K. T. Tait, F. Trouw, Y. Zhao, C. M. Brown, and R. T. Downs, J. Chem. Phys. **127**, 134505 (2007).
[19]N. L. Rosi, J. Eckert, M. Eddaoudi, D. T. Vodak, J. Kim, M. O'Keeffe, and O. M. Yaghi, Science **300**, 1127 (2003).
[20]J. L. C. Rowsell, J. Eckert, and O. M. Yaghi, J. Am. Chem. Soc. **127**, 14904 (2005).
[21]F. M. Mulder, T. J. Dingemans, H. G. Schimmel, A. J. Ramirez-Cuesta, and G. J. Kearley, Chem. Phys. **351**, 72 (2008).
[22]C. M. Brown, Y. Liu, T. Yildirim, V. K. Peterson, and C. J. Kepert, Nanotechnology **20**, 204025 (2009).
[23]P. D. C. Dietzel, P. A. Georgiev, J. Eckert, R. Blom, T. Strässle, and T. Unruh, Chem. Commun. **46**, 4962 (2010).
[24]P. A. Georgiev, A. Albinati, B. L. Mojet, J. Ollivier, and J. Eckert, J. Am. Chem. Soc. **129**, 8086 (2007).
[25]J. M. Nicol, J. Eckert, and J. Howard, J. Phys. Chem. **92**, 7117 (1988).
[26]J. Eckert, F. R. Trouw, B. Mojet, P. Forster, and R. Lobo, J. Nanosci. Nanotechnol. **10**, 49 (2010).
[27]H. G. Schimmel, G. J. Kearlkey, M. G. Nijkamp, C. T. Visser, K. P. de Jong, and F. K. Mulder, Chem.-Eur. J. **9**, 4764 (2003).
[28]P. A. Georgiev, D. K. Ross, A. DeMonte, U. Montaretto-Marullo, R. A. Edwards, A. Ramirez-Cuesta, and D. Colognesi, J. Phys.: Condens. Matter **16**, L73 (2004).
[29]A. Lovell, S. M. Bennington, N. T. Skipper, C. Gejke, H. Thompson, and M. A. Adams, Physica B **385–386**, 163 (2006).
[30]L. Kong, G. Román-Peréz, J. M. Soler, and D. C. Langreth, Phys. Rev. Lett. **103**, 096103 (2009).
[31]M. Xu, Y. Elmatad, F. Sebastianelli, J. W. Moskowitz, and Z. Bačić, J. Phys. Chem. B **110**, 24806 (2006).
[32]M. Xu, F. Sebastianelli, and Z. Bačić, J. Chem. Phys. **128**, 244715 (2008).
[33]M. Xu, F. Sebastianelli, and Z. Bačić, J. Phys. Chem. A **113**, 7601 (2009).
[34]M. Xu, F. Sebastianelli, Z. Bačić, R. Lawler, and N. J. Turro, J. Chem. Phys. **128**, 011101 (2008).
[35]M. Xu, F. Sebastianelli, Z. Bačić, R. Lawler, and N. J. Turro, J. Chem. Phys. **129**, 064313 (2008).
[36]M. Xu, F. Sebastianelli, B. R. Gibbons, Z. Bačić, R. Lawler, and N. J. Turro, J. Chem. Phys. **130**, 224306 (2009).
[37]F. Sebastianelli, M. Xu, Z. Bačić, R. Lawler, and N. J. Turro, J. Am. Chem. Soc. **132**, 9826 (2010).
[38]S. Ye, M. Xu, Z. Bačić, R. Lawler, and N. J. Turro, J. Phys. Chem. A **114**, 9936 (2010).
[39]A. L. R. Bug and G. J. Martyna, Chem. Phys. **261**, 89 (2000).
[40]J. A. MacKinnon, J. Eckert, D. F. Coker, and A. L. R. Bug, J. Chem. Phys. **114**, 10137 (2001).
[41]M. Xu, L. Ulivi, M. Celli, D. Colognesi, and Z. Bačić, Phys. Rev. B **83**, 241403(R) (2011).
[42]M. Xu and Z. Bačić, Phys. Rev. B **84**, 195445 (2011).
[43]H. Stein, H. Stiller, and R. Stockmeyer, J. Chem. Phys. **57**, 1726 (1972).
[44]S. W. Lovesey, *Theory of Neutron Scattering from Condensed Matter* (Oxford University Press, Oxford, 1984), Vol. 1.
[45]M. D. Ward, Science **300**, 1104 (2003).
[46]H. Frost and R. Q. Snurr, J. Phys. Chem. C **111**, 18794 (2007).
[47]D. Zhao, D. Yuan, and H. C. Zhou, Energy Environ. Sci. **1**, 222 (2008).
[48]M. Dinca and J. R. Long, Angew. Chem., Int. Ed. **47**, 2 (2008).
[49]L. J. Murray, M. Dinca, and J. R. Long, Chem. Soc. Rev. **38**, 1294 (2009).
[50]A. Centrone, D. Y. Siberio-Perez, A. R. Millward, O. M. Y. A. J. Matzger, and G. Zerbi, Chem. Phys. Lett. **411**, 516 (2005).
[51]S. Bordiga, J. G. Vitillo, G. Ricchiardi, L. Regli, D. Cocina, Z. Zecchina, B. Arstad, M. Bjorgen, J. Hafizovic, and K. P. Lillerud, J. Phys. Chem. B **109**, 18237 (2005).
[52]J. G. Vitillo, L. Regli, S. Chavan, G. Ricchiardi, G. Spoto, P. D. C. Dietzel, S. Bordiga, and Z. Zecchina, J. Am. Chem. Soc. **130**, 8386 (2008).
[53]S. A. FitzGerald, K. Allen, P. Landerman, J. Hopkins, J. Matters, R. Myers, and J. L. C. Rowsell, Phys. Rev. B **77**, 224301 (2008).
[54]J. L. Belof, A. C. Stern, and B. Space, J. Chem. Theory Comput. **4**, 1332 (2008).
[55]J. L. C. Rowsell, E. C. Spencer, J. Eckert, J. A. K. Howard, and O. M. Yaghi, Science **309**, 1350 (2005).
[56]S. Liu, Z. Bačić, J. W. Moskowitz, and K. E. Schmidt, J. Chem. Phys. **101**, 10181 (1994).
[57]S. Liu, Z. Bačić, J. W. Moskowitz, and K. E. Schmidt, J. Chem. Phys. **103**, 1829 (1995).
[58]I. Matanović, M. Xu, J. W. Moskowitz, J. Eckert, and Z. Bačić, J. Chem. Phys. **131**, 224308 (2009).
[59]Z. Bačić and J. C. Light, Annu. Rev. Phys. Chem. **40**, 469 (1989).
[60]J. L. Belof, A. C. Stern, M. Eddaoudi, and B. Space, J. Am. Chem. Soc. **129**, 15202 (2007).
[61]J. Applequist, J. R. Carl, and K. K. Fung, J. Am. Chem. Soc. **94**, 2952 (1972).
[62]B. Thole, Chem. Phys. **59**, 341 (1981).
[63]P. van Duijen and M. Swart, J. Phys. Chem. A **102**, 2399 (1998).
[64]T. Sagara, J. Klassen, and E. Ganz, J. Chem. Phys. **121**, 12543 (2004).
[65]E. Klontzas, A. Mavradonakis, G. E. Froudakis, Y. Carissan, and W. Klopper, J. Phys. Chem. C **111**, 13635 (2007).
[66]D. A. Gomez, A. F. Combariza, and G. Sastre, Phys. Chem. Chem. Phys. **11**, 9250 (2009).
[67]A. Kuc, T. Heine, G. Seifert, and H. A. Duarte, Theor. Chem. Acc. **120**, 543 (2008).
[68]F. Weigend and R. Ahlrichs, Phys. Chem. Chem. Phys. **7**, 3297 (2005).
[69]A. Hellweg, C. Hättig, S. Höfener, and W. Klopper, Theor. Chem. Acc. **117**, 587 (2007).
[70]C. Hättig and F. Weigend, J. Chem. Phys. **113**, 5154 (2000).
[71]C. Hättig, J. Chem. Phys. **118**, 7751 (2003).
[72]C. Hättig, A. Hellweg, and A. Köhn, Phys. Chem. Chem. Phys. **8**, 1159 (2006).
[73]R. Ahlrichs, M. Bär, M. Häser, H. Horn, and C. Kölmel, Chem. Phys. Lett. **162**, 165 (1989).
[74]B. I. Dunlap, J. W. D. Conolloy, and J. R. Sabin, J. Chem. Phys. **71**, 4993 (1979).
[75]R. J. Renka, ACM Trans. Math. Softw. **10**, 417 (1984).
[76]X.-S. Wang, S. Ma, P. Forster, D. Yuan, J. Eckert, J. López, B. Murphy, J. Parise, and H.-C. Zhou, Angew. Chem., Int. Ed. **47**, 7263 (2008).
[77]Y. Liu, H. Kabbour, C. M. Brown, D. A. Neumann, and C. C. Ahn, Langmuir **24**, 4772 (2008).

[78]F. Nouar, J. Eckert, J. F. Eubank, P. Forster, and M. Eddaoudi, J. Am. Chem. Soc. **131**, 2864 (2009).

[79]T. B. Lee, D. Kim, D. H. Jung, S. B. Choi, J. H. Yoon, J. Kim, K. Choi, and S.-H. Choi, Catal. Today **120**, 330 (2007).

[80]P. Srepusharawoot, C. M. Araujo, A. Blomqvist, R. H. Scheicher, and R. Ahuja, J. Chem. Phys. **129**, 164104 (2008).

[81]L. Kong, Y. J. Chabal, and D. C. Langreth, Phys. Rev. B **83**, 121402 (2011).

[82]V. Buch, S. C. Silva, and J. P. Devlin, J. Chem. Phys. **99**, 2265 (1993).

[83]I. Matanović, N. Došlić, and O. Kühn, J. Chem. Phys. **127**, 014309 (2007).

[84]M. Mališ, I. Matanović, and N. Došlić, J. Phys. Chem. A **113**, 6034 (2009).

[85]M. Dinca, W. S. Han, Y. Liu, A. Dailly, C. M. Brown, and J. R. Long, Angew. Chem., Int. Ed. **46**, 1419 (2007).